FTD-ID(RS)T-0689-91

2

FOREIGN TECHNOLOGY DIVISION

FOLDED LAYER MULTIPLE-PASS CAVITY

by

Xu Yuguang, Yu Qinyue, et. al.

HUMAN TRANSLATION

FTD-ID(RS)T-0689-91 19 November 1991

FOLDED LAYER MULTIPLE-PASS CAVITY

By: Xu Yuguang, Yu Qinyue, et. al.

English pages: 9

Source: Zhongguo Jiguang, Vol. 17, Nr. 10, 1990
pp. 592-595

Country of origin: China

Translated by: SCITRAN
F33657-84-D-0165
Requester: FTD/TTTD /Lt. Cason

GRAPHICS DISCLAIMER

All figures, graphics, tables, equations, etc. merged into this translation were extracted from the best quality copy available.

Accession For		
NTIS GRA&I	☑	
DTIC TAB	☐	
Unannounced	☐	
Justification		
By		
Distribution/		
Availability Codes		
Dist	Avail and/or Special	
A-1		

FOLDED LAYER MULTIPLE-PASS CAVITY
ZHETIESHI CENGZHUANG DUOCHENGQIANG

BY: Xu Yuguang, Yu Qinyue, Lyu Bo, Chen Shouhau and Rong Zhonghua

Abstract: Structure of the folded layered multiple-pass cavity and its image quality are described, uniformity of scanning beam intensity at vertical direction in the middle position of the cavity is discussed, and the high precision result of the reflectance cavity mirror is given:

Key words: folded layered multiple-pass cavity.

J.U. White and D.R. Herriot have done a great deal of research on multiple-pass optical systems and have designed a number of multiple-pass cavities of different structures depending of the use requirements [1,2]. The folded layered multiple-pass cavity presented in this article has the following physical requirements: it must have a light beam with a scanning range of 200mm x 800 mm and with a certain width; the scanning beam in a vertical direction must possess a certain amount of overlapping; the average non-uniformity of the beam intensity along the vertical direction of the central axis of the cavity is to be less than 50 percent. Therefore, it was required that the multiple-pass cavity not only have multiple reflections and good imaging quality of the scanning beam, but it must have an appropriate optical circuit track.

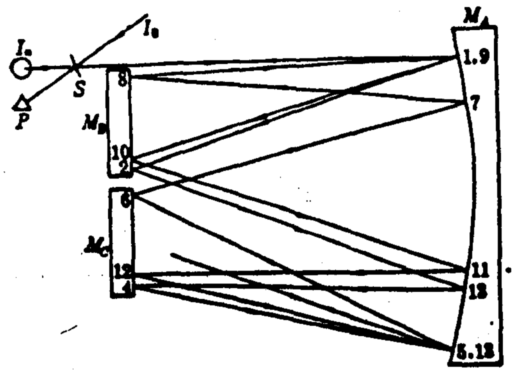

(illus 1)

ILLUSTRATION ONE: THE FOLDED LAYERED MULTIPLE PASS CAVITY

The folded layered multiple-pass cavity we designed is shown in illustration one. In this illustration, at one end of the chamber is a concave mirror M^A, and at the other end of the chamber are two flat mirrors M_B and M_C. The cavity is 1/2 R_A long. The scanning beam is reflected in the cavity in the sequence shown in the illustration. The light beam is reflected a number of times within the cavity, and the image is inverted a number of times. When the direction of light rays transmitted onto the concave mirror M_A overlap with the direction of their radius, they are reflected back along their original route. Illustration two is a photograph of the track of the scanning beam of the folded layered multiple-pass cavity. When the light rays focus on the flat mirror and reflected back off the reflective surface, on the concave mirror M_A, they remain speckles on the convex mirror with the same radius. while on mirrors M_B and M_C, they are alternatively concentrated spots and parallel beam, according to the reflection sequence. Furthermore, when the light beam is reflected back along its original path, the speckles and dots on the flat mirrors exchange places.

Imaging quality is a major characteristic of multiple reflection systems. When the system has little aberration, the image on the mirror always remains 1:1 with multiple inversions, maintain the original structure of the light beam. Hypothetically, when using this optical system, the light transmitted into the system is focussed onto the focal plane of the optical system. When the cavity is 800mm long, a speckle of a diameter of about 10mm will form at L. We know from the theory of aberration that under these conditions, the affect on the image quality is primarily an aberration of an astigmatic difference. We used Young's formula [3] and conducted tracking calculations of the scanning beam with

a computer, determining the astigmatic difference of the exiting beam.

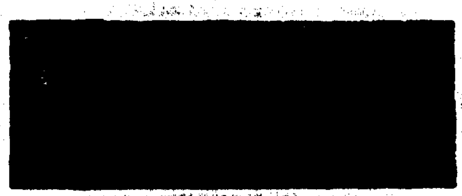

ILLUSTRATION TWO: LIGHT RAY TRACK IN MULTIPLE PASS CAVITY

Assuming that the scanning beam is reflected 137 times in the multiple-pass cavity, the incident conditions of the light beam are as described above. When the scanning height was increased, we observed a change in (x_s-x_t). In illustration three, we can see the graph of (x_s-x_t) corresponding to height of the scanning. When the height of the scanning is increased, the image astigmatic difference very quickly increased. Please not our conditions that H = 200. From the image, we get (x_s-x_t) = 126 mm. The meridian focal line and the isolate out of focus lines were both 1.6mm long. The length of the focal lines affects the size and shape of the speckles of the scanning beam. Considering that these focal lines are the focal lines of the final imaging beam after 137 reflections of the scanning beam within the cavity, the focal lines of any other scanning ray within the cavity would be smaller, this situation totally meets the requirements of the physical conditions.

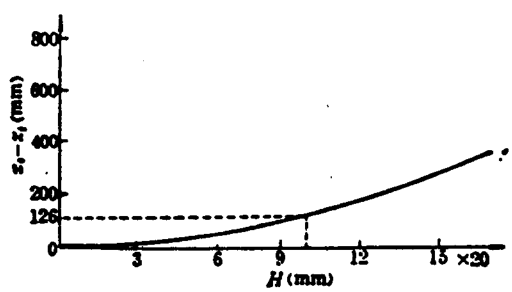

ILLUSTRATION THREE: GRAPH OF SCANNING HEIGHT AND (X_s-X_T)

Assuming that the incidence of the light beam is the same as described above, and with the height of the scan and the number of reflections of the light beam on the mirrors in the cavity remaining the

same, but changing the length of the cavity, also using Young's formula, to calculate the track, we obtain the graph of the correlation of the length L of the cavity and x_m, xt, as is shown in illustration four (a). In illustration four, (b) and (c) are photographs of the speckles and dots on the flat mirrors M_B and M_C when L is 799 and 796 respectively. Although the length of the cavity was only altered by 4/1000nths there is a clear difference between the dots of the two. Therefore, in experiments, it is possible to make suitable adjustments to the length of the cavity to obtain optimum image quality.

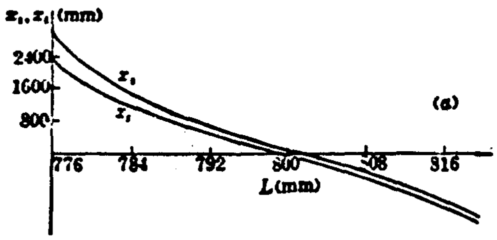

ILLUSTRATION FOUR (A)

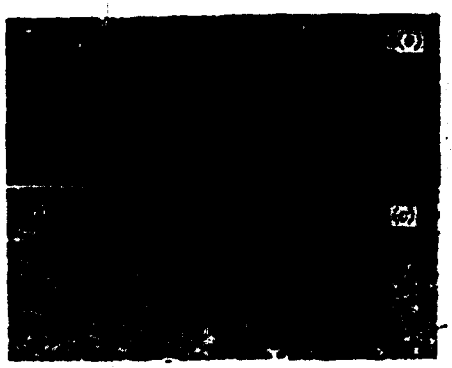

ILLUSTRATIONS FOUR (B) AND (C)

The physics experiment required a thorough overlapping of the scanning beam in the central portion of the multiple-pass cavity, and the average uniformity of the distribution of the light intensity along the vertical direction had to be greater than 50 percent. We know that the intensity of scattered light is directly proportional to the intensity of the light beams. We need only measure the changes in the intensity of the scattered light along the different heights in the chamber, and we can find the changes of the light intensity as the height varies. We used a photoelectric cell at a certain fixed distance from the light beam scanning surface to pick up the scanning light beam scattered light and

had the photo electric cell track along different heights, and recorded changes in the position of the photo electric cell and light intensity signals received simultaneously in two arms of the x-y factor recorder. With the light was focussed on the cavity aperture, and with the speckles on the concave mirror M_a were o10mm, the graph of the correlation between the light intensity I and the height H was as is shown in illustration five. Illustration five (A) shows the relative intensity in different positions along the vertical direction when the light beam is reflected 137 times within the cavity and is reflected along its original route, the is about 52 percent. By adjusting the tilt of the reflective mirrors, and increasing the number of reflections and degree of overlapping within the cavity, the more even the distribution of the light intensity, the nearer the relative intensity comes to 1. With no changes in the incidence of the light beam, if the number of reflections are increased to 177 and 209, the relative intensity increases to 68 and 82 percent respectively as shown in illustrations 5 (B) and 5(C).

ILLUSTRATION FIVE: LIGHT INTENSITY CORRESPONDING TO CHAMBER HEIGHT

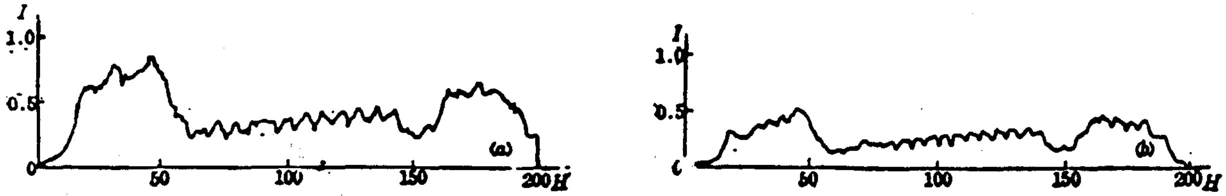

ILLUSTRATIONS FIVE (A) AND FIVE (B)

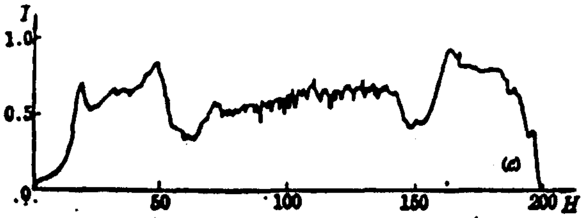

ILLUSTRATION FIVE (C)

naturally, there are limitations to the degree to which the number of reflections of the light beam can be increased. This is restricted by the size of the incident dots. Illustrations six and seven show the light intensity distribution within the cavity and the distribution of light intensity along the central axis of the cavity along the height of the

scan.

ILLUSTRATION SIX: LIGHT INTENSITY DISTRIBUTION WITHIN CHAMBER

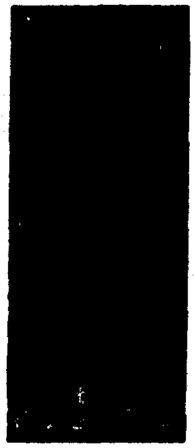

ILLUSTRATION SEVEN: LIGHT INTENSITY ALONG CENTRAL AXIS OF CHAMBER ALONG HEIGHT OF SCAN

The surface reflectivity of the mirrors on either end of the cavity of a multiple-pass cavity directly affects the dissipation and number of reflections within the cavity. The surface loss includes diffraction, absorption, and transmission. When surface reflectivity is greater than 99 percent, the use of the common formula R = 1-T, is no longer accurate. The multiple reflection characteristic of multiple-pass cavities can be used to measure the reflectivity of the mirrors of the cavity to high degree of precision, eliminating the affects of surface diffraction and absorption on the measurements[4].

As illustration one showed, the original light I_o is entered into the multiple reflective system through the spectrum plate S, and adjusting M_m will allow the light beam to return along its original path after scanning, and pass through the spectrum plate S and be transmitted into the integrating globe I_n. The intensity of light picked up by a photoelectric tube and after multiple reflections in the multiple-pass cavity is called I; The incident light intensity I_o passes through the spectrum plate and is measured by the photoelectric receiver. I and I_o can be expressed using the following two formulas:

$$I_o = I_p a_p \quad (1)$$

$$I = I_n a_n \quad (2)$$

In these formulas, I_p and I_n are measured readings of the light beam entering and leaving the multiple-pass cavity. a_p and a_n are set values of I_p and I_n at the detector and the spectrum plate system. Allow R to be the average reflectivity of the flat mirrors, and N be number of reflections of the scan light beam within the cavity. We can now obtain the formulas:

$$I - I_n an = I_p a_p R^N$$

$$I_n/I_p = (a_p/a_n)R^N$$

We now obtain the logarithm:

$$\ln(I_n/I_p) = N\ln r + b \quad (3)$$

In formula (3), $b = \ln(a_p/a_n)$ is a constant. Using the method of the least squares, the slope of the line K is ln R_o $R = e^k$, and we obtain

$$\Delta R = e^k \Delta K = R\Delta K \quad (4)$$

ΔR can be determined by divergence from the line of the experimental data, and calculated from the divergence provided by the fit. Table one displays a group of measurements from the folded layered multiple pass cavity. Using the method of least squares to fit these data, the resultant line is shown in illustration eight.

TABLE ONE:

① 序号	I_p	I_a	② 反射次数N
1	7.6	240	78
2	7.7	210	97
3	7.7	180	121
4	7.5	150	153
5	7.6	127	185

(1) One up sequential number of data batch.

(2) Number of reflections N.

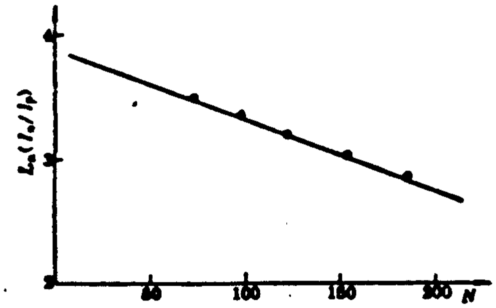

ILLUSTRATION EIGHT

We get the average reflectivity within the cavity as R = 0.99438±4 X 10–5.

The folded layered multiple-pass cavity has few optical elements, is structurally simplistic, is easy to adjust, has good light beam quality, allows for adjusting the number of scans and degree of dot overlapping, and has more uniform distribution of light intensity within the cavity. This provides the opportunity for the laser and the inside of the cavity to interact with a more uniform quality with a certain thickness of plane distribution. The folded layered multiple-pass cavity is a system with more nearly ideal light beam layered scanning.

FOOTNOTES:

1. J. U. White, *J. Opt. Soc. Am.*, 6(5), (1976)
2. D. R. Herriott, H. J. Schulte, *Appl. Opt.*, 4(8), 883~889(1965)
3. Wang Zhijiang, FUNDAMENTALS OF OPTICAL DESIGN THEORY (2nd Edition),

Scientific Press, Beijing, 1985.

4. R. S. Hernicz, D. P. Dewitt, *Appl. Opt.*, 12(10), 2454~2460(1973)

DISTRIBUTION LIST

DISTRIBUTION DIRECT TO RECIPIENT

ORGANIZATION	MICROFICHE
B085 DIA/RTS-2FI	1
C509 BALL0C509 BALLISTIC RES LAB	1
C510 R&T LABS/AVEADCOM	1
C513 ARRADCOM	1
C535 AVRADCOM/TSARCOM	1
C539 TRASANA	1
Q592 FSTC	4
Q619 MSIC REDSTONE	1
Q008 NTIC	1
Q043 AFMIC-IS	1
E051 HQ USAF/INET	1
E404 AEDC/DOF	1
E408 AFWL	1
E410 ASDTC/IN	1
E411 ASD/FTD/TTIA	1
E429 SD/IND	1
P005 DOE/ISA/DDI	1
P050 CIA/OCR/ADD/SD	2
1051 AFIT/LDE	1
CCV	1
P090 NSA/CDB	1
2206 FSL	1

Microfiche Nbr: FTD91C000713
FTD-ID(RS)T-0689-91